

# SIMULATION OF INJECTION EFFICIENCY FOR THE HIGH ENERGY PHOTON SOURCE\*

Z. Duan<sup>†</sup>, J. H. Chen, Y. Y. Guo, D. H. Ji, Y. Jiao, C. Meng, Y. M. Peng, G. Xu

Key Laboratory of Particle Acceleration Physics and Technology,  
Institute of High Energy Physics, Chinese Academy of Sciences, 100049 Beijing, China

## Abstract

A "high-energy accumulation" scheme [1] was proposed to deliver the full charge bunches for the swap-out injection of the High Energy Photon Source. In this scheme, the depleted storage ring bunches are recovered via merging with small charge bunches in the booster, before being refilled into the storage ring. In particular, the high charge bunches are transferred twice between the storage ring and the booster, and thus it is essential to maintain a near perfect transmission efficiency in the whole process. In this paper, major error effects affecting the transmission efficiency are analyzed and their tolerances are summarized, injection simulations indicate a satisfactory transmission efficiency is achievable for the present baseline lattice.

## INTRODUCTION

The baseline lattice (referred to as V2.0 lattice) of the High Energy Photon Source (HEPS) [2] is comprised with 48 hybrid 7BA cells with alternating high- $\beta$  and low- $\beta$  straight sections, and achieves a natural emittance of 34 pm at 6 GeV within a circumference of 1360.4 m. To cope with the small dynamic aperture, the swap-out injection [3] is adopted as the baseline injection scheme. To address the challenges in delivery of the full charge bunches, in particular to prepare the 14.4 nC high charge bunches as required by timing experiments, we proposed a scheme to utilize the booster as a full energy accumulator ring, to recycle and replenish the used bunch in the storage ring [1]. In this injection scheme, the bunch with a high charge is transferred twice, it is essential to maintain a high transmission efficiency in the whole injection cycle. In fact, beam loss primarily manifests as imperfect efficiency during injection into the storage ring and the booster due to various error effects, and could deteriorate as a result of transient beam instability for high-charge bunches. Error effects are analyzed and simulated in this paper, while study of the transient beam instability is reported in a separate paper [4]. These studies were based on the V2.0 lattice of HEPS, similar injection simulations are underway for the new V2.4 $\alpha$  lattice [5] with a smaller dynamic aperture.

## ERROR SOURCES

Different errors in the beam transportation could be categorized into two domains: dynamic errors and static errors. Dynamic errors are fast random variation that lead to pulse-

to-pulse jitter in the injection efficiency, the major contribution is the power supply ripple and glitches of injection and extraction kickers, as well as magnets in the transport lines; the static errors are slow varying errors that could lead to gradual deterioration of injection efficiency, long term drifts of magnet power supply are the major contribution, there are also some residual errors not fully compensated after each injection efficiency optimization.

The effects of different error sources on the injection efficiency, could be approximated by the transverse displacement of the beam centroid relative to the closed orbit at the injection point  $(\Delta x, \Delta x', \Delta y, \Delta y')$ , the effective increase in beam emittance  $(\Delta \epsilon_x, \Delta \epsilon_y)$ , as well as the offset in the beam centroid arrival time and energy  $(\Delta t, \Delta \delta)$ . Contributions to these effects will be described separately.

## Transverse Displacements

The dipole magnetic field errors in the beam transportation process lead to transverse displacements of injected beam centroid, and could be represented by the initial betatron oscillation amplitude of the injected beam centroid  $\Delta u_0 = \sqrt{\beta_{u,0} \Delta A}$ , where  $\Delta A = \gamma_u \Delta u^2 + 2\alpha_u \Delta u \Delta u' + \beta_u \Delta u'^2$  represented the effective Courant-Snyder invariant,  $u$  is  $x$  or  $y$ ,  $\beta_{u,0}$  is the  $\beta$  function at the injection point, and  $(\alpha_u, \beta_u, \gamma_u)$  are the twiss parameters at the error source. Besides, the relative energy offset  $\delta$  between the beam central energy and the energy setting in the transport line magnets, also contribute to a dispersive transverse displacement,  $\Delta u_0 = \Delta D_{u,0} \delta$ , where  $\Delta D_{u,0}$  is the residual dispersion function at the injection point.

Vertical injection and extraction are adopted for both the storage ring and the booster. In the storage ring, the extraction system layout is a mirror of the injection system, with the same hardware specifications. The injection and extraction systems are located in the high- $\beta$  and low- $\beta$  straight sections, respectively<sup>1</sup>. In the booster, to enable beam accumulation at the flat top energy, off-axis injection and extraction are implemented, two kickers with a  $\pi$ -phase advance are adopted for the injection, while a single kicker with four pulsed bumper magnets are adopted for the extraction [6].

The major contributions to the horizontal displacement of the injected beam are the power supply errors of injection and extraction Lambertson magnets as well as bending magnets in the transport line. The bending magnets in the transport line are powered in series, and their power supply share the

<sup>1</sup> This has recently been reversed since it is favored to place a pre-kicker at the high- $\beta$  straight section, and injection in the low- $\beta$  straight section allows a fatter injected beam to relax the dynamic aperture requirement in the horizontal plane.

\* Work supported by Natural Science Foundation of China (No.11605212).  
<sup>†</sup> zhe.duan@ihep.ac.cn

Table 1: Error Budget of Pulsed Magnets

Error source	Error type	Tolerance (peak value)	vertical displacement ( $\mu\text{m}$ rms)
<b>Storage ring injection</b>			180
Booster pulsed bumpers	Amplitude repeatability	0.3%	40
	timing jitter	30 $\mu\text{m}$	
Booster extraction kicker	Amplitude repeatability	0.5%	40
	timing jitter	5 ns	
Storage ring injection kickers	Amplitude repeatability	3%	140
	timing jitter	100 ps	
<b>Booster injection</b>			66
Booster injection kickers	Amplitude repeatability	0.5%	42
	timing jitter	5 ns	
Storage ring extraction kickers	Amplitude repeatability	3%	51
	timing jitter	100 ps	

same specifications as the Lambertson magnets. Assume the power supply ripple and the long term stability (up to 1 week) are both 50 ppm<sup>2</sup>, and add the resultant dynamic and static errors together, this translates to an rms horizontal displacement of 120  $\mu\text{m}$  for the storage ring injection and 80  $\mu\text{m}$  for the booster injection.

In the vertical plane, the major error sources are the power supply errors of pulsed magnets, include the injection and extraction kickers of the storage ring and the booster, as well as the pulsed bumper magnets for booster extraction. In particular, the storage ring injection and extraction kicker systems each contain 8 stripline kickers driven by ultra-fast high voltage pulsers, the R&D progress of these key components are reported in Ref. [7, 8]. In contrast, the booster injection and extraction kickers adopt more conventional technology. The error effects of these kickers include the amplitude repeatability and timing jitter. The allocation of error budget is shown in Table 1. Recent measurements [9] of the homemade fast pulsers of the storage ring kickers show an amplitude repeatability better than 1%, indicating there are some safe margin in the specifications.

In fact, the off-axis injection into the booster has a much larger error tolerance compared to the on-axis injection into the storage ring. In the booster injection efficiency simulation, a much larger transverse displacement setting is adopted compared to the known error sources.

### Effective Beam Emittance Growth

The quadrupole magnetic field errors in the transport line, lead to a mismatch of twiss parameters at the injection point, during the injection, this then manifests as filamentation in the phase space and an increase in rms beam emittances. Therefore, this effect could be approximated with an increase in the beam emittance at the injection point ( $\Delta\epsilon_x, \Delta\epsilon_y$ ). Be-

<sup>2</sup> Recently, the specifications of the ripple and long term stability of these dipole magnet power supplies have been revised to 10 ppm and 40 ppm, respectively.

ides, the residual dispersion functions at the injection point together with the energy spread, also contribute to the beam size and could also be treated as an effective beam emittance growth. After closed orbit correction, the horizontal and vertical emittances in the booster are below 35 nm and 1 nm in most lattice seeds. Take into the effective emittance growth in the transportation process, the horizontal and vertical emittances are taken as 40 nm and 4 nm in the storage ring injection simulation.

The equilibrium beam emittances in the storage ring are about 30 pm and 5 pm, and the beam energy density is very high, there is concern that if sudden kicker failure occur during the extraction, then the beam could hit the septum of the extraction Lambertson magnet and cause significant radiation damage. As a precaution, a pre-kicker system is under study to deflect a bunch before the extraction kicker system fires [10], the bunch is blow up and the energy density is greatly reduced within a few hundred revolutions. Therefore, in the booster injection simulation, the beam emittances are chosen to be 4 nm in both plane to take into account the effect of the pre-kicker.

### Longitudinal Mismatch

The mismatch in the longitudinal phase space includes the error in beam arrival time and the beam central energy, as well as the difference in the equilibrium longitudinal distributions between the storage ring and the booster. The mismatch in the longitudinal phase space leads to filamentation in the injection process and effective increase of longitudinal beam emittance, some large amplitude particles could be out of the RF acceptance and get lost.

The booster RF frequency is three times of the storage ring fundamental RF frequency as a result of engineering choice, the extracted bunch from the storage ring is lengthened due to the 3rd harmonic cavity, and impedance related effects, in particular in the case of 14.4 nC high charge bunch for timing experiments. Therefore, tolerance in the bunch

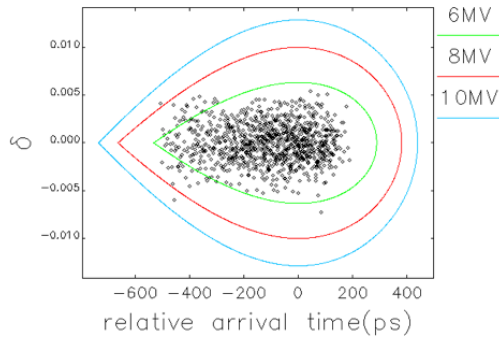


Figure 1: The booster RF acceptance for different total RF voltages (colored lines), and the longitudinal distribution of a 14.4 nC electron bunch extracted from the storage ring (scattered points).

arrival time is more demanding in the booster compared to the storage ring. To be conservative, in the storage ring injection simulation, the rms bunch length and energy spread are chosen to be 120% that of equilibrium values; in the booster injection simulation, the longitudinal beam distribution of a 14.4 nC storage ring bunch is used, as shown in Fig. 1.

The relative error of beam centroid arrival time is primarily caused by the jitter and drift of the relative phase between the booster and the storage ring RF systems. The phase jitter is dominated by the booster RF phase stability, a  $\pm 1$ -degree RF phase stability results in a jitter of beam arrival time of  $\pm 6$  ps. The drift of the relative phase between the storage ring and booster RF systems will be monitored and feedbacked to ensure the drift of beam arrival time is less than 50 ps. In the injection simulation, an rms beam centroid arrival time error of 33 ps is adopted.

The relative energy error of the injected beam is primarily caused by the amplitude and phase errors of the booster and storage ring RF systems. The relative energy error could be reduced in the injection efficiency optimization using the booster extraction energy as the knob. The jitter of storage ring injected beam energy is mainly caused by the dipole magnet power supply ripple at the booster extraction energy, which is small than 0.04%. The drift in the center energy of the storage ring could be monitored by the BPMs in the dispersion bump region and compensated in the orbit feedback system, the energy resolution is within 0.01%. In conclusion, an rms relative energy error of 0.1% is chosen in the injection efficiency simulation.

## INJECTION EFFICIENCY SIMULATIONS

The beam parameters and effective injection error settings are summarized in Table 2. In the injection efficiency simulation with Pelegant [11, 12], 50 random lattice seeds after error introduction and correction are used for the storage ring and the booster. For each random lattice seed, 20 random seeds of effective injection errors are generated to simulate the injection error effects. Realistic RF parameter and ra-

Table 2: Injected Beam Parameters and Effective Injection Error Settings (rms values, truncated at  $3\sigma$ )

	Storage ring injection	Booster injection
<b>Beam parameters</b>		
emittances $\epsilon_x/\epsilon_y$ (nm)	40/4	4/4
rms energy spread $\sigma_\delta$	$1.2 \times 10^{-3}$	$2.0 \times 10^{-3}$
rms bunch length $\sigma_t$ (ps)	50	160
<b>error settings</b>		
transverse displacement $\Delta x/\Delta y$ (mm)	0.12/0.18	0.67/0.33
relative energy error $\Delta_\delta$	$1.0 \times 10^{-3}$	$1.0 \times 10^{-3}$
arrival time error $\Delta t$ (ps)	33.33	33.33

diation damping, as well as a simplified physical aperture setting are adopted in the injection tracking. In each injection simulation, 1000 particles are tracked for 1000 turns, and the particle loss information is recorded. The histograms of beam loss among different injection simulations for the storage ring and the booster are shown in Fig. 2.

The injection efficiency simulations indicate a highly efficient injection is achievable. More detailed start-to-end simulation studies are under way to include all known effects into the efficiency evaluations.

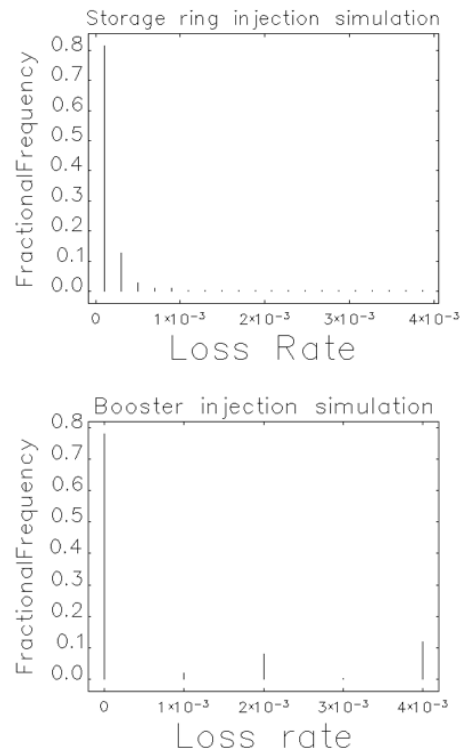


Figure 2: The histograms of beam loss rate during injection into the storage ring(upper plot) and the booster(lower plot).

Content from this work may be used under the terms of the CC BY 3.0 licence (© 2019). Any distribution of this work must maintain attribution to the author(s), title of the work, publisher, and DOI

## REFERENCES

- [1] Z. Duan *et al.*, “The Swap-Out Injection Scheme for the High Energy Photon Source”, in *Proc. 9th Int. Particle Accelerator Conf. (IPAC’18)*, Vancouver, Canada, Apr.-May 2018, pp. 4178–4181. doi:10.18429/JACoW-IPAC2018-THPMF052
- [2] Y. Jiao *et al.*, “The HEPS project”, *J. Synchrotron Rad.* 25, 1611–1618, 2018.
- [3] L. Emery and M. Borland, “Possible Long-Term Improvements to the Advanced Photon Source”, in *Proc. 20th Particle Accelerator Conf. (PAC’03)*, Portland, OR, USA, May 2003, paper TOPA014, pp.256–258.
- [4] Z. Duan *et al.*, “Simulation of the injection transient in-stability for the High Energy Photon Source”, presented at IPAC’19, Melbourne, Australia, May 2019, paper TUPGW053, this conference.
- [5] Y. Jiao *et al.*, “Progress of lattice design and physics studies on the High Energy Photon Source”, presented at IPAC’19, Melbourne, Australia, May 2019, paper TUPGW046, this conference.
- [6] Y. Y. Guo, J. Chen, Z. Duan, Y. Jiao, Y. M. Peng, and G. Xu, “The Injection and Extraction Design of the Booster for the HEPS Project”, in *Proc. 9th Int. Particle Accelerator Conf. (IPAC’18)*, Vancouver, Canada, Apr.-May 2018, pp. 1356–1358. doi:10.18429/JACoW-IPAC2018-TUPMF046
- [7] J.H. Chen *et al.*, “Strip-line kicker and fast pulser R&D for the HEPS on-axis injection system”, *Nuclear Inst. and Methods in Physics Research, A* (2018). doi:10.1016/j.nima.2018.12.009
- [8] L. Wang *et al.*, “A 300 mm Long Prototype Strip-line Kicker For the HEPS Injection System.”, presented at IPAC’19, Melbourne, Australia, May 2019, paper THPRB026, this conference.
- [9] Private communications with G. W. Wang.
- [10] M. Borland, J. C. Dooling, R. R. Lindberg, V. Sajaev, and A. Xiao, “Using Decoherence to Prevent Damage to the Swap-Out Dump for the APS Upgrade”, in *Proc. 9th Int. Particle Accelerator Conf. (IPAC’18)*, Vancouver, Canada, Apr.-May 2018, pp. 1494–1497. doi:10.18429/JACoW-IPAC2018-TUPMK004
- [11] M. Borland, ANL/APS LS-287, Advanced Photon Source, 2000.
- [12] Y. Wang *et al.*, *AIP Conf. Proc.*, vol. 877, p. 241, 2006.